Thermal Protection System Weight Minimization for the Space Shuttle through Trajectory Optimization

FRANK GARCIA JR.*
NASA Johnson Space Center, Houston, Texas

AND

WALLACE T. FOWLER†
The University of Texas at Austin, Austin, Texas

This paper discusses the results of employing a first-order optimization algorithm to the problem of minimizing the weight of the re-entry thermal protection system (TPS) for the space shuttle. Mathematical models of two types of thermal protection systems are derived, a metallic TPS and a reusable surface insulation (RSI) TPS. Optimal entries were generated using maximum orbiter nose temperature as a parameter. Thermal protection system weights were computed for both fixed and variable angles of attack using three-dimensional entry trajectories. Results indicated that variable angle-of-attack entries require less thermal protection system weight than entries at a constant angle of attack (35°) for both systems considered.

Introduction

As presently envisioned, the space shuttle orbiter will employ a reusable skin material for thermal protection during entry.‡ The weight of this thermal protection system (TPS) will depend on the materials of which it is constructed, on the system design, and on the entry trajectories flown by the orbiter. The process of obtaining the material-trajectory combination that produces a minimum weight TPS is very complex.

To accurately represent the skin panel configuration, the orbiter surface is divided into 22 panels on each side of the centerline. However, because the vehicle is symmetrical, each panel is assigned twice the actual area. Then, the weight of each panel is computed separately, and the panel weights are summed to obtain the total TPS weight. A condition of no sideslip is assumed throughout the entry. The orbiter employed in this study used panel area and heating rate data[1] based on a North American-Rockwell delta orbiter (NR 134B).[2] The orbiter surface panel layout is shown in Fig. 1. The aerodynamic characteristics for this vehicle are given in Ref. 2.

To optimize the weight of a particular panel through flight control, it is necessary to know the material or materials of which the panel is constructed, the heating history (i.e., the angle-of-attack history and the orbiter entry trajectory), and the relations between TPS weight, maximum panel temperature and integrated panel heat load. If these relationships are modeled exactly, the task of determining a material-trajectory combination that minimizes total TPS weight employing state-of-the art numerical optimization techniques[3-7] becomes long and improbable, if not impossible. Therefore, the introduction and validation of simplifying assumptions is necessary in order to obtain results that will be of use in choosing an orbiter design. Hopefully, in the refinement process of future studies, the exact degree of approximation made in each assumption can be determined. Such refinements await the development of new methods. However, for the present, only rough validation of simplifying assumptions were made. The assumptions and their validations will be discussed later in the paper.

Presented as Paper 72-997 at the AIAA 2nd Atmospheric Flight Mechanics Conference, Palo Alto, Calif., September 11–13, 1972; submitted September 26, 1972; revision received August 20, 1973.

Index categories: Entry Vehicles and Landers; Spacecraft Temperature Control Systems.

* Aerospace Technologist. Member AIAA.

† Associate Professor, Department of Aerospace Engineering and Engineering Mechanics. Member AIAA.

‡ Since this work was performed, system design and other considerations led to the selection of reusable surface insulation for the space shuttle orbiter TPS.

TPS Material Models

The reusable surface insulation (RSI) TPS is constructed of a rigid fibrous material that can be attached directly to a low temperature structural skin. Optimum local RSI thickness is proportional to the accumulated heat load. The RSI-TPS can withstand a maximum surface temperature of approximately 2500°F, while a columbium metallic system can withstand a maximum local temperature of 2700°F. For this study, RSI was assumed to be directly bonded to titanium skin.

For the RSI system, external surface insulation is not required in those areas where the surface temperatures do not exceed 650°F because the titanium skin is sufficient at this temperature. Surface temperatures are calculated from the relation (neglecting conduction and transient heat capacity terms)

$$T = \dot{q}^{(1/4)}/\varepsilon\sigma \tag{1}$$

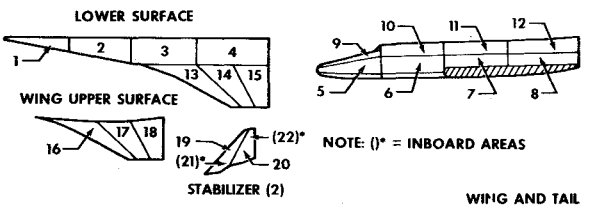

PANEL NUMBER	FUSELAGE AREAS, FT²	PANEL NUMBER	WING AND TAIL AREAS, FT²
1	431	13	1044
2	928	14	860
3	1306	15	846
4	1408	16	894
5	697	17	710
6	1000	18	780
7	671	19	470
8	719	20	416
9	467	21	470
10	1116	22	416
11	1539		
12	1798		

NOTE: TOTAL VEHICLE AREA = 18,986 FT²

Fig. 1 Orbiter panel description.

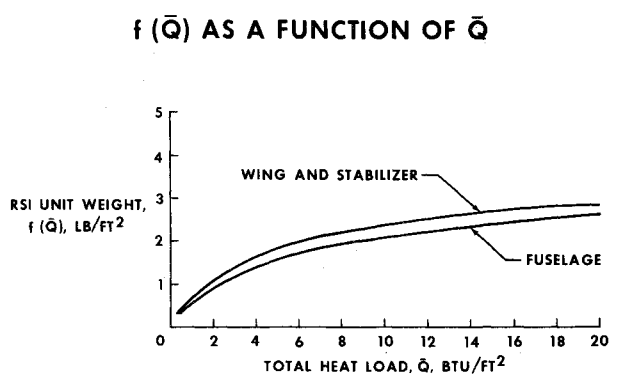

Fig. 2 RSI wt/sq ft vs total heat load.

where T = temperature in °R; $\varepsilon = 0.8$, the surface emissivity; $\sigma = 0.4761 \times 10^{-12}$ Btu/ft²-sec-(°R)⁴, the Stefan-Boltzman Constant; q = the local heating rate in Btu/ft²-sec. The weight of the RSI thermal protection system is given by

$$W_{\text{RSI-TPS}} = W_1 + W_2 \tag{2}$$

where

$$W_1 = \sum_{i=1}^{22} \delta_i L_i A_i \quad \text{with} \quad \delta_i = 1 \quad \text{if} \quad T_{\max_i} \leqq 650°\text{F}$$

$$\delta_i = 0 \quad \text{if} \quad T_{\max_i} \leqq 650°\text{F}$$

and

$$W_2 = \sum_{i=1}^{22} A_i f(\bar{Q}_i)[1-\delta_i]$$

where A = the area of the ith panel; $f(\bar{Q}_i)$ = the weight of insulation per unit area required for the TPS; and $\bar{Q}_i$ = the total heat load per unit in Btu/ft² received by the ith panel over the entire trajectory. When $\delta_i = 1$, the term $L_i A_i$ represents the bare weight (no RSI) of those panels whose peak temperature is less than or equal to 650°F. The term $A_i F(\bar{Q}_i)$ represents the weight of the insulation part of the TPS for the ith panel.

For each panel, the total heat load per unit area $\bar{Q}_i$ determines the weight of the surface insulation per unit area $f(\bar{Q}_i)$ needed. The relationship between $F(\bar{Q}_i)$ and $\bar{Q}_i$ for the RSI-TPS is given in Fig. 2. Note that separate curves are given for fuselage and wing panels.

The total heat load on the ith panel $\bar{Q}_i$ is given by

$$\bar{Q}_i = \int_{t_0}^{t_f} k_i \frac{\tilde{q}}{\dot{q}_r} \dot{q}_R \, dt \tag{3}$$

where $k_i = k_i(\rho, V, \dot{q}_R)$ is a Reynolds number effect factor, $\tilde{q}/\dot{q}_{R_i} = g_i(\alpha)$ is dimensionless surface average heat-transfer rate dependent on angle of attack α for the ith panel, and $\dot{q}_R$ is the stagnation heating rate in Btu/ft²-sec based on a sphere with radius of 1 ft.

Thus, the performance index for minimizing the weight of the RSI-TPS is given by

$$W_{\text{RSI-TPS}} = = \sum_{i=1}^{22} A_i f \int_{t_0}^{t_f} k_i \frac{\dot{q}}{\dot{q}_R} dt[1-\delta_i] + W_1 \tag{4}$$

where W_1 is given by Eq. (2).

For the metallic TPS, panels can be selected from several different metals, depending on the peak entry temperature (Fig. 3). Soft insulation is placed behind surface panels to protect the low temperature surface. The thickness of insulation is proportional to the accumulated heat load. For panels that do not experience peak temperatures in excess of 650°F, a structural skin backed by a layer of insulation is assumed. The weight of a given panel depends on the material of which the panel is made and the thickness of the insulation required on the panel. The choice of material for a panel depends on the maximum temperature to be experienced by the panel [Eq. (1)], and the insulation thickness depends on the total heat load experienced by the panel.

The weight of the metallic TPS can be expressed as

$$W_{M\text{-TPS}} = \sum_{i=1}^{22} (W_{1i} + W_{2i}) \tag{5}$$

where $W_{1i} = L_i A_i$ is the product of the area A_i of the ith panel and a function $L_i = L_i(T_{i\text{-max}})$ of the maximum temperature $T_{i\text{-max}}$ experienced by the ith panel; and where $W_{2i} = A_i f(\bar{Q}_i)[1-\delta_i]$ is a term completely analogous to the insulation weight term for the RSI-TPS [Eqs. (2) and (3)] except that a different set of constants are used in the function $f(\bar{Q}_i)$ for the metallic TPS. Note that for panels whose peak temperatures are less than or equal to 650°F, as in the RSI-TPS, a minimum weight penalty is assessed to the TPS weight.

Because the weights of both the RSI and metallic TPS depend on combinations of functions and/or constraints involving maximum panel surface temperatures and total heat load, and because of the nature of the functions in Fig. 2, a straightforward application of standard optimization techniques to the problem of minimizing TPS weight is very difficult. It is impossible to know, before a trajectory iterate, what the peak temperatures on the various panels will be and it is impossible to know how to specify beforehand which metal to use for any given panel. To overcome a portion of this difficulty, a state variable inequality constraint was placed in the stagnation heating rate $\dot{q}_R$ which kept the maximum panel surface temperature below a specified level. This in effect, defined the maximum surface temperature for the hottest panels beforehand and defined the metal of which the hottest panels were to be constructed.

Computational Models

If the function $f(\bar{Q}_i)$ is approximated by a function that is of second order or higher in $\bar{Q}_i$, then the performance index is not of a proper form for immediate optimization by standard variational methods. In such a case, a new state variable must be introduced for each term of order higher than 1 in $\bar{Q}_i$ in the expression for $f(\bar{Q}_i)$, and other simplifications must be made before the problem is in a form that can be handled by standard variational methods. Approximations of $f(\bar{Q}_i)$ vs $\bar{Q}_i$ that are linear in $\bar{Q}_i$ cause the introduction of no new state variables and are very desirable if such approximates produce satisfactory results. The accuracy of any such approximations produce satisfactory results. The accuracy of any such approximation must be checked carefully before it is accepted into a TPS model because inaccuracies here could produce either an inadequate TPS or an overweight TPS, both of which are undesirable.

The approximations of $f(\bar{Q}_i)$ that were investigated will now be described. Various polynomial approximations to the curves of

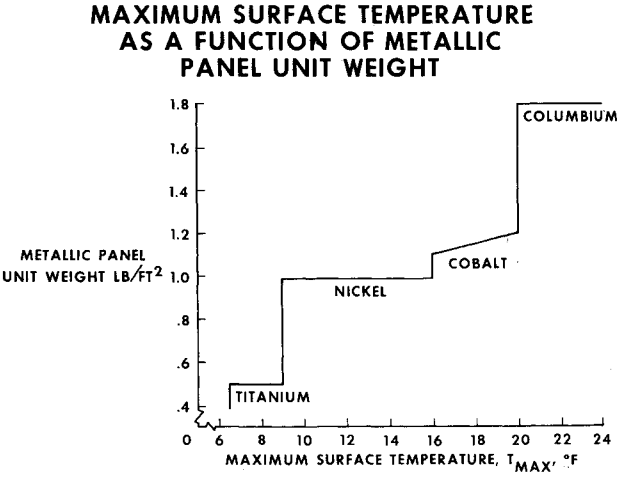

Fig. 3 Metallic TPS wt/sq ft vs maximum surface temperature.

Fig. 2 were attempted, keeping in mind that the higher the order of the approximating polynomial, the more difficult the optimization problem became. Polynomials of order up to four were fitted to the curves of Fig. 2 but it was finally decided that a linear approximation would suffice because on a typical trajectory, most of the heat loads for individual panels lie between 2000 and 8000 Btu/ft^2, and a linear fit works well in this range.

The heat transfer ($\tilde{q}/\dot{q}_R$) data given for the delta orbiter configuration of Fig. 1 were in the form of numerical values for each panel at $\alpha = 30$ and 53°. Thus, a straight-line fit of ($\tilde{q}/\dot{q}_R$) as a function of angle of attack α is the best that can be had from the given data. The turbulent heating and transition Reynolds number are based on the results presented in Ref. 8. The model used was

$$\tilde{q}/\dot{q}_R = m_i\alpha + b_i \tag{6}$$

If $f(\bar{Q}_i)$ is approximated by a straight line of the form

$$f(\bar{Q}_i) = C_1\bar{Q}_i + C_2 \tag{7}$$

then the substitution of Eqs. (3, 6, and 7) into W_2 of Eq. (2) leads to an expression for the insulation weight in the form

$$W_2 = \sum_{i=1}^{22} A_i C_1[1-\delta_i]\int_{t_0}^{t_f} k_i(m_i\alpha + b_i)\dot{q}_R\,dt + \sum_{i=1}^{22} A_i C_2 \tag{8}$$

A further attempt to simplify TPS weight predictions was made in which constant angle-of-attack simulations were carried out using an entry simulation program that provided panel TPS weight and maximum temperatures for arbitrary trajectories. This simulation program did not model $f(\bar{Q}_i)$ vs $\bar{Q}_i$ as a linear function, and its results indicated that a majority of the TPS weight was accumulated while the flow was laminar. This suggested an assumption that $k_i = 1$ (independent of the Reynolds number) be used throughout the optimization process. Table 1 shows the Reynolds numbers at which the flow underwent transition from laminar to turbulent for the various panels on the skin of the orbiter as calculated in the simulation program.

Table 1 Transition Reynolds numbers for orbiter panels

Reynolds number at which transition occurred	Panels on which flow transitioned at this Reynolds number
3500	4
7000	3
12000	2, 6
15600	15
19400	1, 5, 9, 10, 11, 12, 14, 19, 20
24000	7, 8, 13, 16, 17, 18, 21, 22

Using this last assumption and rearranging terms in Eq. (8), the form for W_2 now becomes

$$W_2 = K_1\int_{t_0}^{t_f}\alpha\dot{q}_R\,dt + K_2\int_{t_0}^{t_f}\dot{q}_R\,dt + K_3 \tag{9}$$

where

$$K_1 = C_1\sum_{i=1}^{22} A_i m_i[i-\delta_i], \quad K_2 = C_1\sum_{i=1}^{22} A_i m_i[1-\delta_i],$$

and

$$K_3 = C_2\sum_{i=1}^{22} A_i$$

for constant α trajectories, Eq. (9) reduces to

$$W_2 = (K_1\alpha + K_2)\int_{t_0}^{t_f}\dot{q}_R\,dt + K_3 \tag{10}$$

Thus, for trajectories characterized by constant angle of attack, this insulation model of the TPS-trajectory interaction yields the result that a minimum weight TPS will be obtained along the trajectory that minimizes the quantity

$$(K_1\alpha + K_2)\int_{t_0}^{t_f}\dot{q}_R\,dt + K_3 + W_1$$

For the variable angle-of-attack trajectories, the minimum weight TPS will be obtained along the path that minimizes the quantity

$$K_1\int_{t_0}^{t_f}\alpha\dot{q}_R\,dt + K_2\int_{t_0}^{t_f}\dot{q}_R\,dt + K_3 + W_1$$

It is important to note at this point that the constants K_1 and K_2 differ for the two TPS material models and that the term W_1 depends on which TPS is being considered, as discussed previously.

Simulations and Results

The procedure for producing minimum TPS weight trajectories at constant angle of attack (35°) and variable angle of attack involved two programs: a gradient trajectory optimization program and an entry simulation program. Both programs were modified to produce the information necessary for TPS optimization. The linearization and laminar flow assumptions were used only in the trajectory optimization program. The optimal control programs produced by the optimization program were used as input for the entry simulation program that produced detailed TPS panel weights and temperatures for both the metallic and the RSI thermal protection systems. There was a small difference in the trajectories produced with the two programs, which is probably because of differences in the way in which the two programs carry out numerical integrations. The differences were less than 1% of the variables involved and are negligible.

The trajectory optimization program was used to produce a trajectory that started from the following state at $t = 0$:

h = 400,000 ft	Latitude = 0°
V_{REL} = 24,055.102 fps	Longitude = 0°
γ_{REL} = −0.984°	Heading = 0° (East)

This state defines initial conditions for entry from an equatorial orbit. From such an orbit, crossrange can be specified simply by constraining the terminal value of the latitude. The terminal conditions chosen for all cases were

h_f = 80,000 ft	Latitude = 17.6486° (1100 naut mile crossrange)
V_f = free	Longitude = free
γ_f = free	Heading = free
	t_f = free

The inequality constraints that were imposed were $20° \leqq \alpha \leqq 53°$ for trim capability limits; $\dot{h} \leqq 0\ (t_0, t_f)$ to control phugoids; and $\dot{q}_R \leqq \dot{q}_{R\text{-max}}(t, t)$ to limit the maximum temperature that always occurs on the nose panel where $\dot{q}_{R\text{-max}}$ was always chosen so that the maximum material temperature limits were not exceeded. Several constant angle-of-attack optimal entries at $\alpha = 35°$ and

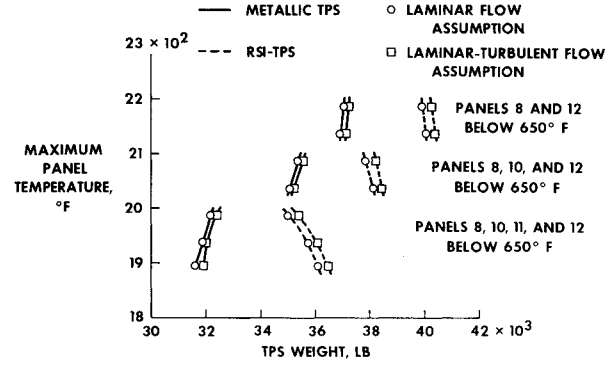

Fig. 4 TPS weights for entries at angle of attack of 35°.

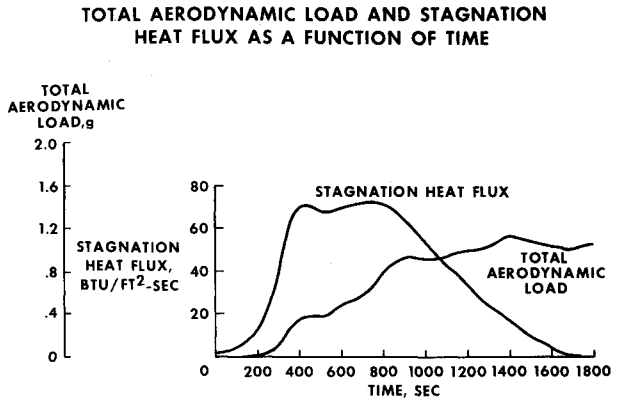

Fig. 5a

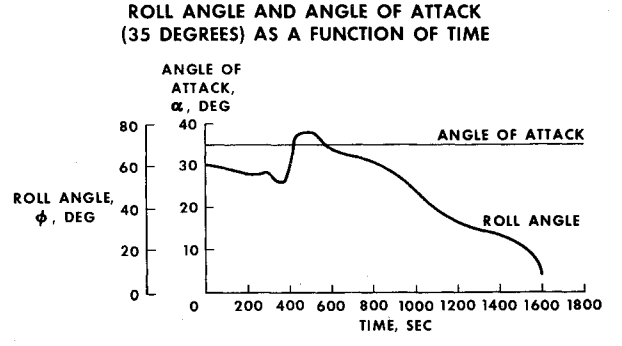

Fig. 5b

Fig. 5 Typical trajectory for $\alpha = 35°$

$$65 \leqq \dot{q}_R \leqq 106 \text{ Btu/ft}^2\text{-sec}$$

were run and Fig. 4 shows the results of both the laminar flow and the laminar-turbulent flow assumptions. Although these results justify the assumption that $k_i \cong 1$ only for $\alpha = 35°$, this assumption was also made for variable angle of attack re-entries.

By varying the constraint levels on $\dot{q}_R$, it was possible to determine trajectories for which TPS weight became smaller or larger. Small values of $W_{M\text{-TPS}}$ were achieved by making $\dot{q}_R$ small (a cool entry). The trajectories having small metallic TPS weights had large heat loads $\bar{Q}$ and thus large values for W_2. However, the weight savings from the small values of W_1 more than compensated for the increased weight caused by the increased heat loads, $\bar{Q}$. By requiring $\dot{q}_R$ to be increased, $\bar{Q}$ could be reduced resulting in smaller values for W_2.

Figure 4 shows the TPS weight results for both the RSI and metallic systems vs the maximum allowable surface temperature T_{max} (controlled by the $\dot{q}_R$ constraint). From Fig. 3, it can be seen that the range of $\dot{q}_R$ chosen allows selection of certain types of metallic panels for the TPS on any given trajectory. The TPS weights are shown for both laminar and laminar-turbulent assumptions as pointed out earlier. The discontinuities seen as maximum temperature increases are caused by individual panel temperatures going above 650°F.

Figure 5a shows the heating rate $\dot{q}_R$ and the acceleration in g's experienced by the shuttle vs time during the entry for a typical constant angle-of-attack optimal entry. Figure 5b shows the bank angle ϕ and the angle of attack vs time (α is constant in this case) for the same constant angle-of-attack optimal entry. Note from Figure 5a the constant $\dot{q}_R$ and total aerodynamic load characteristics of the trajectory. Because there was no constraint on the aerodynamic load, its constant characteristics are likely caused by the crossrange requirements and the constraint on $\dot{h}$.

The minimization of variable angle-of-attack trajectories involved a change in the performance index of the system. For

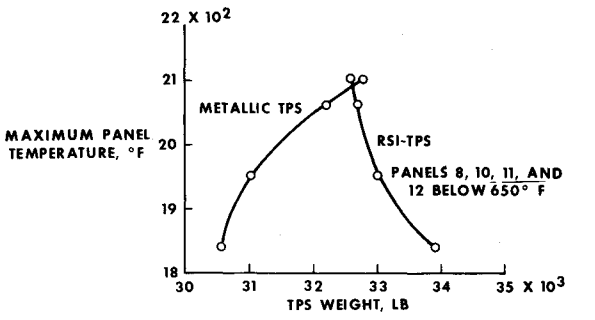

Fig. 6 TPS weights for entries at variable angle of attack.

the variable angle-of-attack case, Eq. (9) gives the weights W_2 for both TPS models. If a new state variable, W_{TPS}, is introduced, its defining differential equation and initial condition are

$$W_{TPS} = (K_1 \alpha + K_2)\dot{q}_R \tag{11}$$
$$W_{TPS}(t_0) = K_3$$

In addition to these relations, the trajectory optimization program required partial derivatives of the right-hand side of Eq. (10) with respect to the state and control variables in the problem. The two control variables used in the trajectory optimization program are pitch angle θ and bank angle ϕ. The angle of attack α is a function of θ and γ (flight-path angle). When minimizing TPS weight for variable angle-of-attack entries using this mode, the variable

$$\int_{t_0}^{t_f} \alpha \dot{q}_R \, dt$$

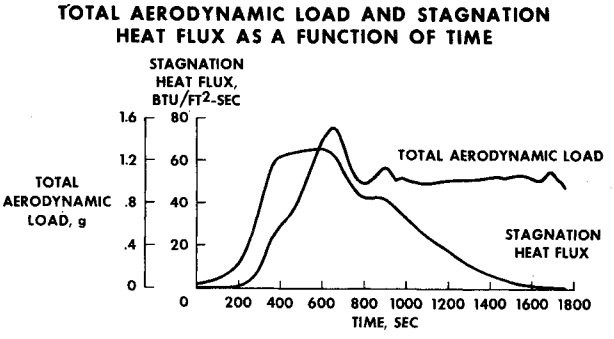

Fig. 7a

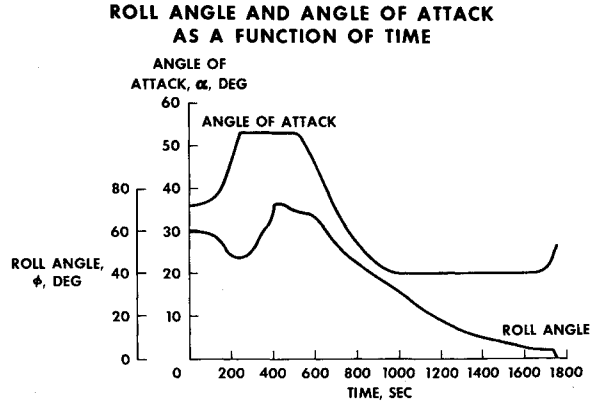

Fig. 7b

Fig. 7 Typical re-entry trajectory with variable angle of attack.

must be used as a state variable because the definition of W_{TPS} involves this variable. The initial value of this variable is zero.

The initial conditions for variable angle-of-attack entries were the same as those used for the fixed angle-of-attack entry. Four variable angle-of-attack trajectories were run employing different heating rate constraints

$$(54 \leqq \dot{q}_{R\text{-max}} \leqq 82 \text{ Btu/ft}^2\text{-sec})$$

The resulting laminar TPS weights for both RSI and metallic systems are shown as a function of T_{max} in Fig. 6. Note that no discontinuities appear as temperature increases because no crossover of the 650°F boundary occurs on any of the panels.

From Fig. 3, it can be seen that the range of $\dot{q}_{R\text{-max}}$ values was chosen to select certain types of metallic panels in the TPS (for a particular trajectory). As the maximum allowable value of $\dot{q}_R(T_{max})$ decreases, the metallic TPS becomes more and more desirable. For high values of $\dot{q}_R$, the RSI-TPS is more desirable. For high values of $\dot{q}_R$, the metallic TPS becomes very heavy because the metals having higher weight per unit area must be used.

Figure 7a shows $\dot{q}_R$ and g's experienced during a typical variable angle-of-attack optimal entry; Fig. 7b shows bank angle ϕ and angle of attack α for the same trajectory. Note from Fig. 7a that the trajectory is characterized by a segment in which $\dot{q}_R$ is approximately constant, followed by a segment in which the g level experienced is approximately constant (aerodynamic load, not constrained). This same type of behavior was noted for the constant angle-of-attack cases.

Conclusions

The trajectories presented in Figs. 5 and 7 are typical of those that can be produced by a gradient optimization procedure for fixed and variable angle-of-attack entries. The results obtained when angle of attack is used as a control indicates that variable angle-of-attack entries will produce lower TPS weights than will the fixed angle-of-attack entries for the TPS types considered. The amount of decrease of TPS weight will depend on the specific angle of attack chosen for the fixed angle-of-attack entries and the angle-of-attack range chosen for the variable angle-of-attack entries. Although this study indicates that variable angle-of-attack trajectories are desirable from a minimum TPS standpoint, other design considerations might dictate the use of constant angle of attack data for TPS design. (For example, constant α is a very easy back-up control mode.)

Because of the highly constrained nature of the problem, it seems possible that simple suboptimal control schedules can be devised that produce TPS weights lying between the fixed angle-of-attack and variable angle-of-attack values. The constant $\dot{q}_R/g$ characteristics of the trajectories obtained in this study suggest that a good suboptimal guidance scheme might be to fly a constant $\dot{q}_R$ level segment followed by a constant g segment.

References

[1] Lockman, W. K. and de Rose, C. E., "Aerodynamic Heating of a Space Shuttle Delta-Wing Orbiter," TM-X-62057, Aug. 1971, NASA.

[2] Space Shuttle Aerodynamics Group, "NR Space Shuttle Program—Aerodynamics Design Data Book—Volume II Delta-Wing Orbiter," SD70-414, Aug. 1970, North American Rockwell Corp., El Segundo, Calif.

[3] Kelly, H. J., Kopp, R. E., and Moyer, H. G., "Successive Approximation Techniques for Trajectory Optimization," *Proceedings of the IAS Symposium on Vehicle Systems Optimization*, Institute of Aerospace Sciences, Garden City, New York, Nov. 1961.

[4] Bryson, A. E. and Denham, W. F., "A Steepest-Ascent Method for Solving Optimum Programming Problems," *Journal of Applied Mechanics*, June 1962.

[5] Blanton, H. E., ed., "Three-Dimensional Trajectory Optimization Study, Part I—Optimum Programming Formulation," Rept. BR-3136-1, Sept. 25, 1964, Raytheon Co., Lexington, Mass.

[6] Hague, D. S., "Three-Degree-of-Freedom Problem Optimization Formulation," USAF Rept. FDL-TDR-64-1, Vol. 3, Pt. 1, Oct. 1964, Flight Dynamics Lab., Wright-Patterson Air Force Base, Ohio.

[7] Stein, L. H., Matthews, M. L., and Frenk, J. W., "STOP—A Computer Program for Supersonic Transport Trajectory Optimization," CR-793, May 1967, NASA.

[8] Strouhal, G. and Curry, D. M., "TPS Trade Studies on Ablators and Reusable Surface Insulation," *Proceedings of the NASA Space Shuttle Conference*, San Antonio, Texas, April 1972.